

Title	Bone Marrow Dose in Fast Neutron Irradiation Calculated From Geometrical Bone Structure Part 2
Author(s)	山本, 修
Citation	日本医学放射線学会雑誌. 1966, 26(5), p. 446-453
Version Type	VoR
URL	https://hdl.handle.net/11094/14779
rights	
Note	

Osaka University Knowledge Archive : OUKA

<https://ir.library.osaka-u.ac.jp/>

Osaka University

Bone Marrow Dose in Fast Neutron Irradiation
Calculated From Geometrical Bone Structure
(Part 2)

By

Osamu Yamamoto

Department of Radiation Biology, Research Institute for Nuclear
Medicine and Biology, Hiroshima University,
Hiroshima, Japan

幾何学的骨構造から計算される速中性子骨髄線量 (その 2)

広島大学原爆放射能医学研究所障害基礎部門

山 本 修

(昭和41年12月21日受付)

14.1MeV 速中性子照射骨髄のエネルギー吸収の算定に際し、前報に与えられた式を反跳陽子のエネルギーとその散乱角との関係を考慮して補正し、さらに組織中の水素以外の他の構成成分の寄与をも考慮にいった。

速中性子照射による組織中のエネルギー吸収は、その吸収の形においてX線、 γ 線、 α 線とは異った特性をもつ。

マウスとラツテの骨髄エネルギー吸収量の比較をX線、 γ 線、速中性子についておこなつた。組織エネルギー附与平衡値にたいする骨髄吸収量の相対値は次のようになった。X線、 γ 線、速中性子について、マウスではそれぞれ1.09, 1.01および0.92となり、ラツテではそれぞれ1.06, 1.01および0.93と算出された。

Introduction

Spiers¹⁻³⁾ has developed a method of calculating energy absorption in the soft tissue medium adjacent to the layer of bone. This method was expanded by Epp et al.⁴⁾ and Sinclair⁵⁾ as applied to X-rays and gamma-rays. Kononekno⁶⁾ and Charlton and Cormack^{7,8)} have also reported on a method of calculating energy dissipation in finite cavities by electrons together with the problem of alpha radiation.

In previous papers the author^{9,10)} attempted an estimate of the marrow doses of protons recoiled by 14.1 MeV fast neutrons. The results of the calculations showed that the energy absorption curve differed from that of X-rays, being lower near the first bone-bone marrow interface. The necessity for further correction or modification to obtain a better approximation was presented.

The corrections were made and in this paper the differences in energy absorption of bone marrow among some kinds of radiation to small animals will be discussed.

Modification I

Previously reported calculations of energy absorption from recoil protons were based on methods

given by Spiers. The resulting curve of energy absorption versus distance from that of X-rays. However, the previous report ignored the energy dependence of the protons on scattering angle. This is the essence of the present modification I.

For a neutron-proton collision, the proton energy has been represented by $E_N \cos^2 \theta$ in the laboratory coordinates. An incident flux of neutrons below about 20 MeV, monoenergetic at E_N , will produce protons distributed uniformly in energy up to E_N upon hydrogenous material⁽¹¹⁾.

The relation between proton energy and the range (R_T) has been already given in previous paper (Part 1). In this paper author tried to reconsider the proton range. As illustrated in Fig. 1, proton energy will be dissipated within the range of $R_T \cos \theta$ (Table 1), because the proton disperses having the scattering angle, θ . Thus $R_T \cos \theta$ was substituted for R_T which has been used in a previous paper (Part 1) and the equations were revised in this paper as follows:

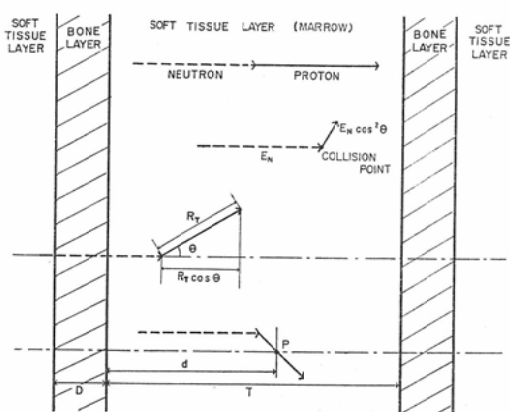


Fig. 1. The illustration of aspects of protons recoiled by neutrons.

Table 1. Proton energy (E) and the corresponding proton range (R_T) and $R_T \cos \theta$ value.

E (MeV)	R_T (μ)	$R_T \cos \theta$ (μ)
0.706	13.8	—
2.118	80.4	3
3.530	192.1	16
4.942	342.6	52
6.354	534.7	129
7.766	763.1	267
9.178	1024.7	485
10.590	1321.6	792
12.002	1640.4	1220
13.414	2041.1	1842

1. The energy absorption at point P contributed by protons produced secondarily in the finite layer of soft tissue (marrow), d microns in thickness:

$$D_T = \sum N_T E \left[1 - f \left(\frac{d}{R_T \cos \theta} \right) \right] \text{ ergs/cm}^3/n$$

2. The energy absorption at point P contributed by protons produced secondarily in the finite layer of bone, D microns in thickness:

$$D_B = \Sigma \frac{N_B E}{\rho} f\left(\frac{d}{R_T \cos \theta}\right) - \Sigma \frac{N_B E}{\rho} f\left(\frac{d + \rho D}{R_T \cos \theta}\right) \text{ ergs/cm}^3/\text{n}$$

3. The energy absorption at point P contributed by protons produced secondarily in the semi-infinite layer of soft tissue on the other side of the bone layer:

$$D_T' = \Sigma N_T E f\left(\frac{d + \rho D}{R_T \cos \theta}\right) \text{ ergs/cm}^3/\text{n}$$

where

N_T = number of protons of initial energy E (ergs) produced in soft tissue per cubic centimeter per unit flux of neutron.

N_B = number of protons of initial energy E (ergs) produced in bone per cubic centimeter per unit flux of neutron.

ρ ratio of stopping power of bone to that of soft tissue.

R_T = range in soft tissue of a proton of energy E.

θ recoil angle of proton.

$$f\left(\frac{d}{R_T \cos \theta}\right) = 1 + \left(\frac{d}{R_T \cos \theta}\right) \left[\ln\left(\frac{d}{R_T \cos \theta}\right) - 1 \right]$$

$$f\left(\frac{d + \rho D}{R_T \cos \theta}\right) = 1 + \left(\frac{d + \rho D}{R_T \cos \theta}\right) \left[\ln\left(\frac{d + \rho D}{R_T \cos \theta}\right) - 1 \right]$$

The energy absorption at point P can be obtained by the summation of above three expressions.

Modification II

For the calculation of energy absorption from 14.1 MeV neutrons the chief contribution made by protons has been discussed in the previous paper and in the last paragraph in this paper. It is also necessary to consider other components in tissue, though their contribution is smaller than that of hydrogen nucleus.

There are four common elements—hydrogen, oxygen, nitrogen and carbon—in the constitution of soft tissue^{9,12}. As for percent values of energy deposition in wet tissue, Randolph¹³ lists 69.5% as elastic scattering for hydrogen, 4.2% as elastic scattering and 26.3% as inelastic scattering for carbon, nitrogen, oxygen and others. Therefore, the contribution of other components excluding hydrogen accounts for 30.5% of all the energy absorption in soft tissue. The author employed this value, 30.5%, for the purpose of further correcting the estimation of energy absorption.

The average recoil energy can be given approximately by $2AE_0/(A+1)^2$ (where A is the mass number of atom and E_0 is the initial energy of neutron). The recoil energy with neutrons for the other constituent atoms excluding hydrogen will be extremely small, because carbon, oxygen and nitrogen have higher mass number than that of hydrogen. Really the ranges of the nuclei of the three constituents other than hydrogen come to be negligibly shorter than that of hydrogen for elastic or inelastic scattering.

One should rather take up, however, the effects of nuclear transformation products. One knows $O^{16}(n,\alpha)C^{13}$ reaction in this process. The reaction product, 7 MeV alpha-particles are the second most important ones for the contribution of energy absorption, and the range, 65 microns in soft tissue, is also the second one in length. But the contribution for energy absorption is only 6.8% which is estimated from Randolph's value. Even if one would use following presumption, the estimation error comes to be only a few percent within the range of 65 microns.

It was presumed, therefore, that the energy contribution of the constituents other than hydrogen would be same throughout the marrow. Thus their energy contribution, $(44.46 \text{ ergs/cm}^3/\text{n} \times 30.5/69.5)$, was added equally to the energy contribution of hydrogen. The value $44.46 \text{ ergs/cm}^3/\text{n}$ is the tissue equilibrium value contributed by only recoil protons.

The relation between bone layer thickness, marrow layer thickness and average energy absorption is shown in Table 2 and Fig. 2 as the result of estimations. When the bone layers are semi-infinite and 50 microns in thickness, the relation between the average energy absorption and the thickness of bone marrow layer can be compared with the uncorrected curves described in the previous paper and with those of X-rays and gamm-rays as shown in Fig. 3.

Table 2. The average energy absorption in different distance by unmodified and modified estimations ($\times 10^{-8} \text{ ergs/cm}^3/\text{n}$).

Soft tissue layer (μ) Bone layer (μ)		10	50	100	200	400	1000	2500
		50	Unmod.	41.87	42.72	43.42	44.29	45.21
Mod. I	39.44		39.93	40.76	41.67	42.57	43.39	44.00
Mod. II	58.95		59.44	60.27	61.18	62.08	62.90	63.51
100	Unmod.	38.85	39.91	40.92	42.21	43.60	45.13	46.39
	Mod. I	36.64	37.47	38.60	39.94	41.31	42.66	43.68
	Mod. II	56.15	56.98	58.11	59.45	60.82	62.17	63.19
200	Unmod.	35.09	36.42	37.70	39.43	41.42	43.83	45.82
	Mod. I	33.58	34.66	36.07	37.81	39.71	41.73	43.23
	Mod. II	53.09	54.17	55.58	57.32	59.22	61.24	62.74
500	Unmod.	29.30	30.56	32.47	34.99	37.94	41.69	44.89
	Mod. I	30.00	31.31	32.95	35.10	37.58	40.50	42.74
	Mod. II	49.51	50.82	52.46	54.61	57.09	60.01	62.25
1000	Unmod.	27.59	29.31	31.02	33.50	36.66	41.03	44.61
	Mod. I	28.62	30.00	31.72	34.01	36.73	40.03	42.55
	Mod. II	48.13	49.51	51.23	53.52	56.24	59.54	62.06
Semi-infinite	Unmod.	27.27	29.01	30.75	33.27	36.50	40.96	44.58
	Mod. I	28.45	29.85	31.58	33.90	36.65	40.00	42.53
	Mod. II	47.96	49.36	51.09	53.41	56.16	59.51	62.04

Unmod.: The values before the modifications.

Mod. I: The values obtained after the modification I.

Mod. II: The values obtained after the modification II.

Application to Physical Models

Epp et al.⁴⁾ has presented the table of physical model for mouse and Sinclair⁵⁾ has also dealt with mouse and rat. Using their tables, an average path length across bone or marrow in parallel was estimated respectively as follows. In this estimation it was presumed that Category I had a sandwich form, Category II had a cylindrical form, and Category III and Category IV had a form as if hollow balls were piled up.

For Category I, \bar{T} and \bar{D} are as original of models.

For Category II:

Average path length across the cylindrical cavity

$$\bar{T} = \frac{2}{r} \int_0^r \sqrt{r^2 - x^2} dx$$

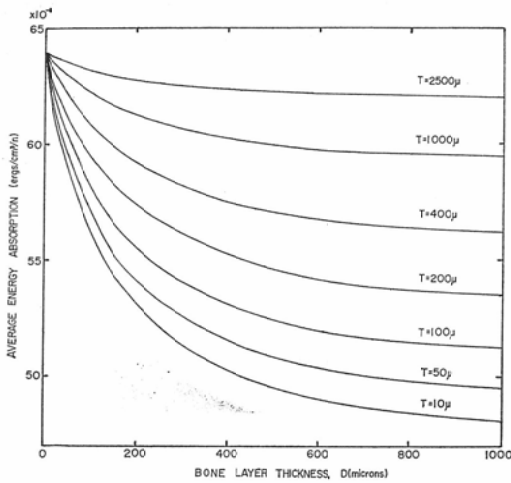


Fig. 2. The relation between bone layer thickness and average energy absorption.

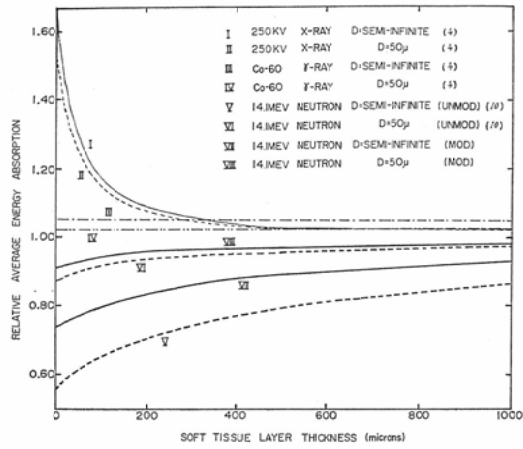


Fig. 3. Average energy absorption in soft tissue (marrow) between various thicknesses of bone.

Average path length across the bone wall

$$\bar{D} = \frac{1}{r} \int_0^r \sqrt{R^2 - x^2} dx - \int_0^r \sqrt{r^2 - x^2} dx$$

where r= cylindrical cavity radius and R=r+ bone wall thickness.

For Category III and Category IV:

Average path length across the spherical cavity

$$\bar{T} = \frac{2}{\pi r^2} \int_0^{\pi} \int_0^r \sqrt{r^2 - x^2} dx d\theta$$

Average path length across the bone wall

$$\bar{D} = \frac{1}{\pi r^2} \left[\pi r^2 \int_0^{\pi} \int_0^R \sqrt{R^2 - r^2} dx + \pi R^2 \int_0^{\pi} \int_0^r \sqrt{R^2 - r^2} dx - \pi \int_0^{\pi} \int_0^R x^2 dx - \int_0^{\pi} \int_0^r \sqrt{r^2 - x^2} dx d\theta \right]$$

where r=spherical cavity radius and R=r+ bone wall. thickness. The diagrams determining r and R

Table 3. Bone and bone marrow models and, \bar{T} and \bar{D} values for mouse and rat.

Category	Components	Mouse			Rat		
		Model ⁽¹⁾	\bar{T} (μ)	\bar{D} (μ)	Model ⁽²⁾	\bar{T} (μ)	\bar{D} (μ)
I	Ribs, clavicle, sternum, pelvis	Marrow layer 300 μ thick between bone layers 150 μ thick.	300	150	Marrow layer 600 μ thick between bone layers 200 μ thick.	600	200
II	Limb bones	Cylinder marrow 900 μ in diameter, bone wall 350 μ .	710	400	Cylinder marrow 1450 μ in diameter, bone wall 600 μ .	1140	680
III	Vertebrae	Lattice marrow spheres 200 μ in diameter, bone wall 80 μ .	130	80	Lattice marrow spheres 300 μ in diameter, bone wall 1000 μ .	200	110
IV	Skull	Spheres of marrow 170 μ in diameter, embedded in bone of total thickness 500 μ .	110	270	Spheres of marrow 300 μ in diameter, embedded in bone of total thickness 850 μ .	200	460

were induced simply from physical models given as a constant averaged, and r and R were not used in dual role of variable.

From \bar{T} and \bar{D} values (Table 3) estimated by the above formulae, each average energy absorption for categories I—IV can be obtained using Table 2 and Fig. 2. In Table 4 the energy absorption value for each category and the weighted average energy absorption of the bone marrow in the whole body are shown. The comparison among some radiations can be made in Table 5. For X-rays and gamma-rays the energy absorption based on \bar{T} and \bar{D} values are shown with the relative values (the marrow energy absorption/the tissue equilibrium energy absorption) in the table in comparison to those presented by Epp et al. and Sinclair.

Table 4. Average doses to various bone marrow categories for 14.1 MeV fast neutron ($\times 10^{-8}$ ergs/cm³/n).

Category	Mouse		Rat	
	Total body ⁴⁾ marrow (%)	Dose	Total body ⁵⁾ marrow (%)	Dose
I	47	59.1	20	60.1
II	20	59.2	38	60.1
III	21	59.3	33	59.1
IV	12	54.8	9	54.9
Weighted average	58.6		59.3	

Table 5. Average marrow dose and relative value to soft tissue equilibrium value for various radiations to mouse and rat.

Radiation	Mouse		Rat	
	Average dose	Relative value to soft tissue equilibrium value	Average dose	Relative value to soft tissue equilibrium value
X-ray (250 kV)	98.8 (98.6*) ergs/cm ³ /r	1.088 (1.086*, 1.087**)	95.9 ergs/cm ³ /r	1.056 (1.066**)
γ -Ray (Co-60)	94.4 (94.0*) ergs/cm ³ /r	1.011 (1.006*, 1.01**)	94.8 ergs/cm ³ /r	1.014 (1.011**)
Neutron (14.1 MeV)	58.6×10^{-8} ergs/cm ³ /n	0.916	59.3×10^{-8} ergs/cm ³ /n	0.927

* These values were given by Epp et al. for 250 kV X-ray and Co-60 gamma-ray.

** These values were given by Sinclair for 200 kV X-ray and Co-60 gamma-ray.

Tissue equilibrium value: X-ray (250kV) 90.8 ergs/cm³/r⁴⁾, γ -ray (Co-60) 93.4 ergs/cm³/r⁴⁾, neutron (14.1MeV) 64.0×10^{-8} ergs/cm³/n.

Result and Discussion

Theoretical estimations for the bone marrow energy absorption from various radiations have been done by some workers. The author has dealt with the marrow energy absorption from protons recoiled by 14.1 MeV fast neutrons in Part 1 and Part 2 of his report. Recoil protons do not scatter backward from the collision point. But they scatter forward in direction of 2π having different energies with scattering angles. Based on this characteristic of protons, the equations given in Part 1 were modified in Part 2. Moreover, in this paper, Part 2, the energy contribution of the other constituents excluding hydrogen was

also considered using Randolph's table as reference.

According to the estimated results, the distribution of energy absorption in marrow for fast neutrons differs in type from those for X-rays, gamma-rays and alpha-rays. In Fig. 4 the energy absorption figures for fast neutrons and X-rays are shown. The relation thus obtained was applied to mouse and rat in determining their marrow doses using physical models presented by Epp et al. and Sinclair. Considerable differences were noted between the marrow absorption doses estimated for X-rays, gamma-rays and fast neutrons as shown in Table 6.

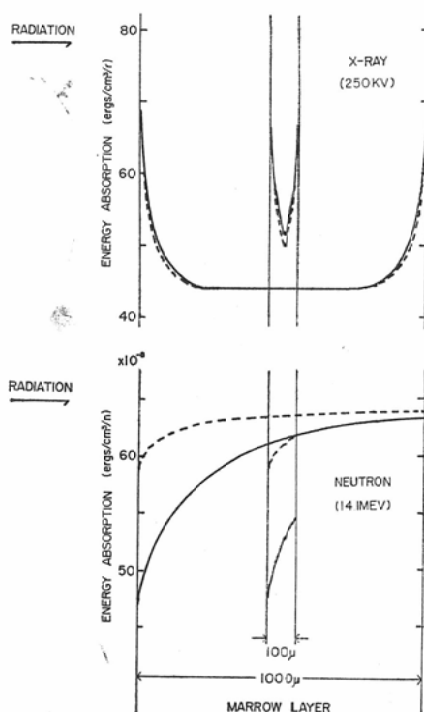


Fig. 4. Energy absorption in marrow (—D=Semi-infinite,D=50 μ).

Table 6. The relative marrow energy absorption values and the differences for X-ray, gamma-ray and fast neutron.

	X-ray	γ -Ray	Neutron	Neutron $\sim\gamma$ -Ray	Neutron \sim X-ray
Mouse	1.09	1.01	0.92	0.09	0.17
Rat	1.06	1.01	0.93	0.08	0.13

Thus, differences in damage effects by the exposure of these radiations can be expected as a matter of course. If there are two primary mechanisms of lethality, one caused by intestinal damage and the other by marrow damage, the probability of lethality from bone marrow damage will be greater for X-rays irradiation than for neutrons irradiation when exposed same doses considered relative value to soft tissue equilibrium dose. Really in the case of X-rays the death affected mainly with marrow damage has been observed at about 15th day after irradiation, while the death with intestinal damage at a few day after

irradiation. In the case of fast neutron the death time is striking at a few day after irradiation¹⁴⁾. It likes that the marrow damage was cut down because of the dose reduction of marrow surrounded by bone. Recently such a tendency as this theoretical result has been histologically observed by Hirose¹⁵⁾.

Summary

For the estimation of energy absorption in bone marrow with 14.1 MeV fast neutrons, the equations given in the previous paper were revised with consideration given to scattering angle and energy of proton.

The contributions of other constituents excluding hydrogen in tissue for the energy absorption were added to the energy distribution of protons.

The energy absorption in tissue by fast neutron irradiation have a characteristic different from that of X-rays, gamma-rays and alpha-rays with respect to absorption pattern.

The marrow energy absorptions were compared on mouse and rat for X-rays, gamma-rays and fast neutrons. Relative values to tissue equilibrium values were 1.09, 1.01 and 0.92 on mouse for X-rays, gamma-rays and fast neutrons respectively, and 1.06, 1.01 and 0.93 on rat respectively.

Acknowledgement

The author wishes to thank Dr. H. Yoshinaga and Dr. K. Takeshita for many helpful discussions and suggestions during this work.

A report based on this study was given at the 22nd General Meeting of Radiological Society of Japan, Osaka, April 4, 1963.

References

- 1) Spiers, F.W.: Effective atomic number and energy absorption in tissues. *Brit. J. Radiol.* **19**, 52—63 (1946).
- 2) Spiers, F.W.: The influence of energy absorption and electron range on dosage in irradiated bone. *Brit. J. Radiol.* **22**, 521—533 (1949).
- 3) Spiers, F.W.: Dosage in irradiated soft tissue and bone. *Brit. J. Radiol.* **24**, 365—369 (1951).
- 4) Epp, E.R., Woodard, H.Q. and Weiss, H.: Energy absorption by the bonemarrow of the mouse receiving whole-body irradiation with 250 Kv X-rays or cobalt-60 gamma rays. *Rad. Res.* **11**, 184—197 (1959).
- 5) Sinclair, W.K.: The relative biological effectiveness of 22 Mevp X-rays, cobalt-60 gamma rays, and 200 Kvep X-rays. *Rad. Res.* **16**, 369—383 (1962).
- 6) Kononenko, A.M.: Calculation of the intensity of the alpha-radiation dose arising a radioactive substance distributed inside the organism. *Biofizika* **2**, 98—117 (1957).
- 7) Charlton, D.E. and Cormack, D.V.: Energy dissipation infinite cavities. *Rad. Res.* **17**, 34—49 (1962).
- 8) Charlton, D.E. and Cormack, D.V.: A method for calculation the alpha-ray dosage to soft tissue-filled cavities in bone. *Brit. J. Radiol.* **35**, 473—477 (1962).
- 9) Yamamoto, O., Sawada, S. and Yoshinaga, H.: Fast neutron absorption dose estimated from the elemental constitution of bone marrow of small animals. *Nipp. Act. Radiol.* **23**, 141—145 (1963).
- 10) Yamamoto, O.: Bone marrow dose in fast neutron irradiation calculated from geometrical bone structures (Part 1). *Nipp. Act. Radiol.* **23**, 146—156 (1963).
- 11) Moyer, B.J.: Neutron physics of concern to the biologist. *Rad. Res.* **1**, 10—22 (1954).
- 12) Rossi, H.H., Hurst, G.S. and Hungerford, H.L.: Intercomparison of fast neutron dosimeters. *Nucleonics* **13**, 46—47 (1955).
- 13) Randolph, M.L.: Energy deposition in tissue and similar materials by 14 MeV neutrons. *Rad. Res.* **7**, 47—57 (1957).
- 14) Sawada, S.: Differences of lethal effects between neutron and X-ray single exposure on mice. *Proc. Hiroshima Uni. RINMB* **3**, 31—34 (1962).
- 15) Hirose, F.: Acute injuries with 14.1 MeV fast neutron irradiation in mice. Presented at IAEA Symposium (On biological effect of neutron irradiations), Brookhaven, October 10, 1963.